



3D-QSAR and molecular docking studies of selective agonists for the thyroid hormone receptor β

Juan Du, Jin Qin, Huanxiang Liu, Xiaojun Yao*

Department of Chemistry, Lanzhou University, Lanzhou 730000, China

ARTICLE INFO

Article history:

Received 16 December 2007
Received in revised form 10 March 2008
Accepted 10 March 2008
Available online 16 March 2008

Keywords:

Thyroid hormone receptor β
CoMFA
CoMSIA
Docking

ABSTRACT

Three-dimensional quantitative structure–activity relationship (3D-QSAR) models were developed using comparative molecular field analysis (CoMFA) and comparative molecular similarity analysis (CoMSIA) on a series of agonists of thyroid hormone receptor β (TR β), which may lead to safe therapies for non-thyroid disorders while avoiding the cardiac side effects. The reasonable q^2 (cross-validated) values 0.600 and 0.616 and non-cross-validated r^2 values of 0.974 and 0.974 were obtained for CoMFA and CoMSIA models for the training set compounds, respectively. The predictive ability of two models was validated using a test set of 12 molecules which gave predictive correlation coefficients (r^2_{pred}) of 0.688 and 0.674, respectively. The Lamarckian Genetic Algorithm (LGA) of AutoDock 4.0 was employed to explore the binding mode of the compound at the active site of TR β . The results not only lead to a better understanding of interactions between these agonists and the thyroid hormone receptor β but also can provide us some useful information about the influence of structures on the activity which will be very useful for designing some new agonist with desired activity.

© 2008 Elsevier Inc. All rights reserved.

1. Introduction

Nuclear receptors (NRs), composed of a family of ligand-dependent transcription factor, closely associate with the regulation of expression of special genes on body growth and development, cell differentiation and many physiological and metabolic process. This family includes many members, such as steroids hormone, retinoic acid, thyroid hormone, vitamin D, etc. [1]. Many of these NRs are potential targets for the therapy of a variety of diseases [2–6]. The thyroid hormone receptors are important members of the NRs super family exerting profound effects on growth, development, and homeostasis in mammals [1]. They regulate important genes in intestinal, skeletal, and cardiac muscles, liver, and the central nervous system, influence overall metabolic rate, cholesterol and triglyceride levels, and heart rate, and affect mood and overall sense of well being. Some effects of thyroid hormones may be therapeutically useful in non-thyroid disorders if adverse effects can be minimized or eliminated. These potentially useful features include weight reduction for the treatment of obesity [7], cholesterol lowering for treating hyperlipidemia [8–10], amelioration of depression, and stimulation of bone formation in osteoporosis.

There are mainly two subtypes of the thyroid hormone receptors, α (TR α) and β (TR β), expressed from two different genes. TR α was reported to mediate the effects of thyroid hormones on the heart, and in particular on the heart rate and rhythm, while most actions of the hormones on the liver and other tissues are mediated more through the β -forms of receptor [11,12]. Up to now, there are many reported thyroid ligands [13–17]. The group of Malm synthesized several series of selective ligands for TR β [18–24], based on the structures of endogenous thyroid receptor hormones 3,5,3',5'-tetraiodo-L-thyronine (T4) and 3,5,3'-triiodo-L-thyronine (T3). These thyroid hormone receptor ligands could lead to safe therapies for non-thyroid disorders while avoiding the cardiac side effects and, therefore, could be used as a short term supplemental therapy to the conventional treatments [25,26].

A number of quantitative structure–activity relationship (QSAR) models, as well as structure–activity relationships (SARs) [27–30] based on these compounds using different molecular descriptors have been validated. Vedani et al. developed the satisfactory 4D–6D QSAR models to study the selective thyroid ligands by using Quasar and Raptor software [29,30]. These models can identify the structural requirements needed for high binding affinity of ligands to TR β and, therefore, offered some useful clues in structural modifications for medicinal chemists. To date, there are no three-dimensional quantitative relationships (3D-QSAR) studies of these ligands reported. Compared with traditional QSAR models derived from molecular descriptors, 3D-QSAR models can give

* Corresponding author. Tel.: +86 931 891 2578; fax: +86 931 891 2582.
E-mail address: xjyao@lzu.edu.cn (X. Yao).

more information about the influence of the agonist conformation on the activity which will be useful for the further structural modification. In addition, combination use of docking study with 3D-QSAR can provide more information on the interaction mode between the agonist and the receptor. In this paper, we have performed 3D-QSAR studies on a series of selective agonist ligands [18,19,21,22] for the TR β 1 using comparative molecular field analysis (CoMFA) [31,32] and comparative molecular similarity analysis (CoMSIA) [33] combined with molecular docking approach. The aims of this research include two aspects. The first one is to explore the binding mode of these agonists with TR β 1. The other one is to obtain 3D-QSAR models, which cannot only be used in rapidly and accurately predicting the activities of new designed agonists, but also provide some beneficial information in structural modifications for designing new agonists with desired binding affinities with TR β 1.

2. Methodology

2.1. Dataset

A data set of 61 compounds act as agonist of TR β taken from Refs. [18,19,21,22] was employed in this study. The structures of all compounds and their biological activity expressed as pIC₅₀ were listed in Table 1. The whole dataset was divided into two sets, 49 compounds in training set and 12 in test set (asterisked molecules in Table 1). The training set was used to construct 3D-QSAR models and the test set was used for the models validation.

2.2. Molecular modeling and alignment

All the molecular modeling and calculations were performed by SYBYL 6.9 molecular modeling package [34] on a Silicon

Table 1
Dataset structure and experimental activity

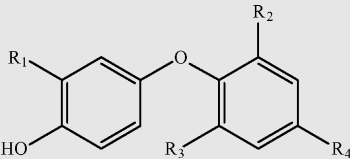

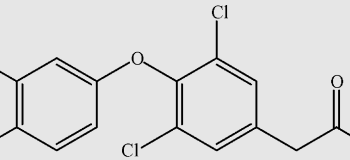
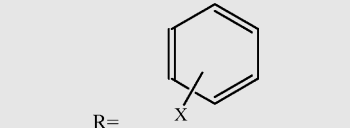
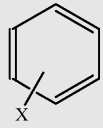
Structure	NO.	Substituents	pIC ₅₀
	1	R4	
	2	–CH ₂ CH(NH ₂)CO ₂ H	9.59
	3	–CH ₂ CO ₂ H	10.32
	4	–CH ₂ CH(NH ₂)CO ₂ H	9.96
	5	–(CH ₂) ₂ CO ₂ H	10.72
 <p>1,2,4: R₁ = R₂ = R₃ = I; 3,5–10: R₁ = Isopropyl; 3: R₂ = R₃ = I; 5–7: R₂ = R₃ = Br; 8–10: R₂ = R₃ = Cl</p>	6	–CO ₂ H	8.68
	7*	–CH ₂ CO ₂ H	10.02
	8*	–CO ₂ H	7.68
	9	–CH ₂ CO ₂ H	8.96
	10	–(CH ₂) ₂ CO ₂ H	9.82
	11*	X	
	12	–H	8.54
	13	2–CF ₃	8.47
	14	3–CF ₃	9.03
	15	4–CF ₃	7.17
	16	3–Et	9.70
	17	3–Isopropyl	8.40
	18	3–Ph	7.68
	19	3–OCH ₃	7.96
	20*	3–OCHF ₂	9.11
	21	3–OCF ₃	8.47
	22	2–OH	7.30
	23	3–OH	7.12
	24	4–OH	7.06
	24	6.86	
 <p>R=</p> 	25	R=	7.39
	26*	R=	6.91
	27	R=	7.17
	28*	R=	7.55
	29*	R= n-C ₆ H ₁₁ X	8.11

Table 1 (Continued)

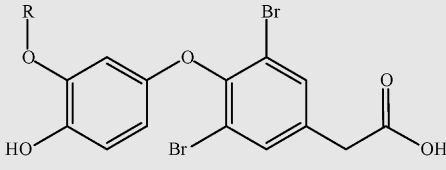
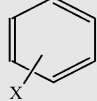
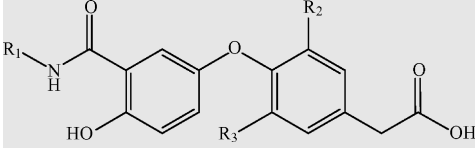
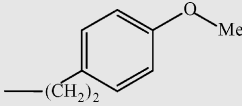
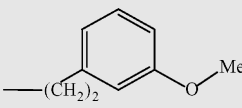
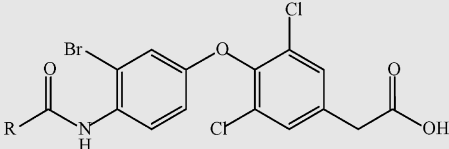
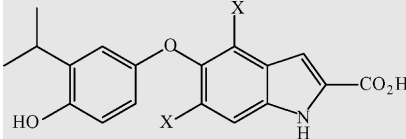
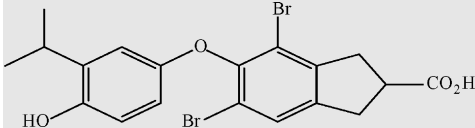
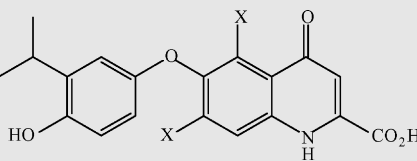
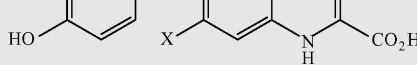
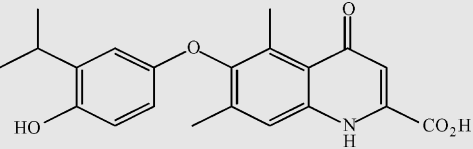
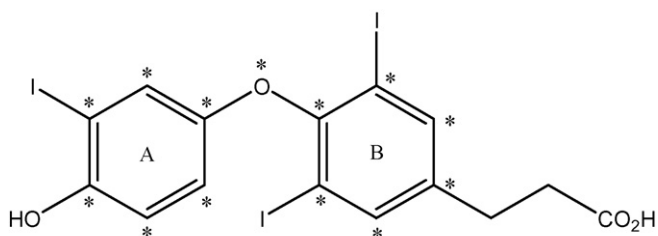
Structure	NO.	Substituents	pIC ₅₀
	30	–H	8.22
	31	2-CF ₃	8.12
	32	3-CF ₃	8.96
	33	4-CF ₃	8.02
	34 ⁺	3-Ph	7.22
	35	2-OH	7.08
	36	3-OH	7.33
	37	4-OH	8.22
R = 	38	R1 –Ph	7.46
	39	–Bz	8.38
	40	–(CH ₂) ₂ Ph	9.21
	41 ⁺	–(CH ₂) ₃ Ph	8.17
	42 ⁺	–(CH ₂) ₄ Ph	7.74
	43		7.43
	44		8.32
	45		8.07
	46 ⁺ 47	–CH ₂ CHPh ₂	9.33 7.17
	48	–(CH ₂) ₂ Ph	8.46
	49	R	
	50	–CH ₂ CH ₃ –CH(CH ₃) ₂	6.85 7.74
	51	–CH(CH ₃)CH ₂ CH ₃	8.37
	52	–CH(CH ₃)CH ₂ CH ₂ CH ₃	7.33
	53	–CH(CH ₂ CH ₃) ₂	7.80
	54	–CH(CH ₂ CH ₂ CH ₃) ₂	7.35
	55	X	
	56	–Br	9.55
	57	–Cl	10.22
		–	8.07
	58	–Br	7.29

Table 1 (Continued)

Structure	NO.	Substituents	pIC ₅₀
	59	–Cl	6.06
	60	–Me	6.62
	61*	–	7.82

* Test set.

**Fig. 1.** Structure of the template molecule (compound no. 4), the asterisks indicate the atoms selected as the common substructure.

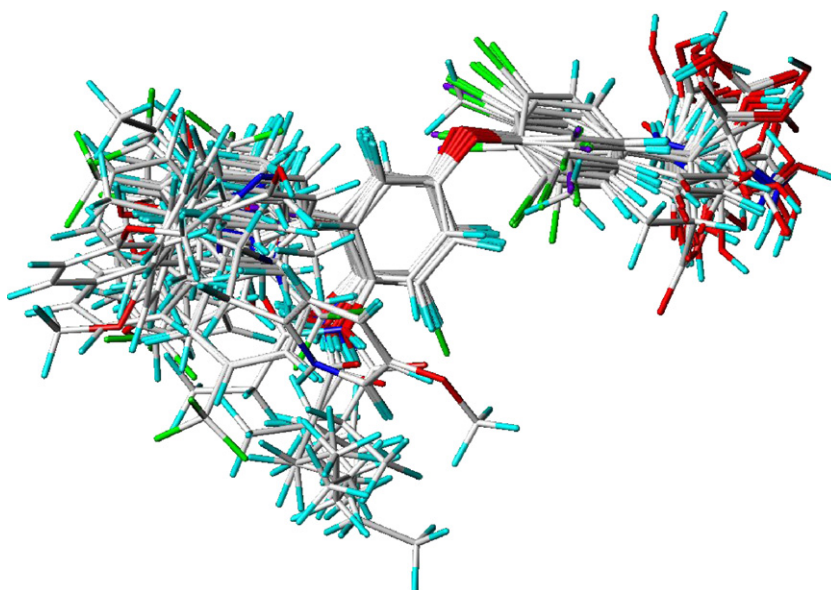
Graphics O2 workstation running under the IRIX 6.5 operating system. Energy minimizations were performed using the Tripos force field with a distance-dependent dielectric and Powell gradient algorithm with a convergence criterion of 0.01 kcal/mol. Partial atomic charges were calculated using Gasteiger–Hückel method.

In the 3D-QSAR studies, alignment rule and bioactive conformation selection are two important factors to construct reliable models. The most active compound 4 was selected as a template. Molecules alignment was performed using DATABASE ALIGNMENT

in SYBYL with the common substructure asterisked in compound 4 (Fig. 1). The resulting alignment was shown in Fig. 2.

2.3. Molecular docking

The AutoDock (Version 4.0) [35] program was chosen to dock the compound 4 into the active site of the thyroid hormone receptor β and explore the binding mode between the compound 4 and the receptor. The 3D coordinates of the thyroid hormone receptor β in complex with ligand were taken from the Brookhaven Protein Databank (PDB code: 1NAX) [18]. AutoDock tools (ADT) were used to prepare the ligand, protein (deleting all water molecules, adding polar hydrogens and loading Kollman United Atoms charges) and also to perform docking calculations. A grid box with the dimensions $60 \times 50 \times 50$ points was constructed around the binding site, based on the location of the co-crystallized ligand. All bond rotations and torsions for the ligand were automatically set in the ADT. Considering the flexibility of the protein during the ligand–receptor interaction process, the four chief interaction residues Arg 282, Arg 320, Asn 331 and His 435 were defined as flexible residues in the docking process. The Lamarckian genetic algorithm (LGA) procedure was employed and the docking runs were set to 50. The rest of the parameters were taken as default.

**Fig. 2.** The alignment of all the compounds in training set.

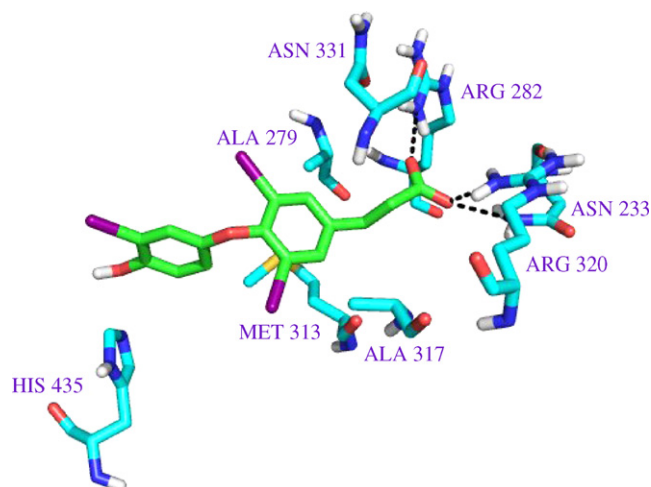


Fig. 3. The three-dimensional representation of interactions between ligand 4 and the TRβ at the active site of TRβ produced using the PyMOL program developed by DeLano [39].

2.4. CoMFA and CoMSIA models generation

The CoMFA descriptors, steric (Lennard–Jones potentials) and electrostatic (Coulomb potentials) field energies were probed using sp^3 carbon probe atom with a +1 charge and a van der Waals radius of 1.52 Å using default settings in SYBYL. The steric and

electrostatic interactions were calculated using the Tripos force field with a distance-dependent dielectric constant at all intersections on a regularly spaced grid of 2.0 Å. The grid box was generated automatically by the Sybyl/CoMFA outline and extended 4.0 Å units in the X, Y, and Z directions beyond the dimensions of aligned molecules. The minimum σ (column filter) was set to 2.0 kcal/mol. The cutoff value of 30 kcal/mol was adopted.

In the CoMSIA model, five physicochemical properties, namely steric, electrostatic, hydrophobic, hydrogen-bond donor and acceptor fields, were calculated using a sp^3 carbon probe atom with a +1 charge atom and a radius of 1.0 Å placed at regular grid spacing of 2 Å and a similar lattice box as used in CoMFA calculations. CoMSIA similarity indices (A_F) for a molecule j with atom i at a grid point q are calculated by Eq. (1):

$$A_{F,k}^q(j) = - \sum_{i=1}^n w_{probe,k} w_{ik} e^{-\alpha r_{iq}^2} \quad (1)$$

where w_{ik} is the actual value of the physicochemical property k of atom i , and $w_{probe,k}$ is the value of the probe atom. A Gaussian type distance dependence is used between the grid point q and each atom i of the molecule, where r represents the distance. The default value of 0.3 was used as the attenuation factor (α).

2.5. PLS regression analysis

The CoMFA and CoMSIA descriptors were used as independent variables, and pIC_{50} values were used as the target variables in partial least squares (PLS) [36,37] regression analyses to derive 3D-

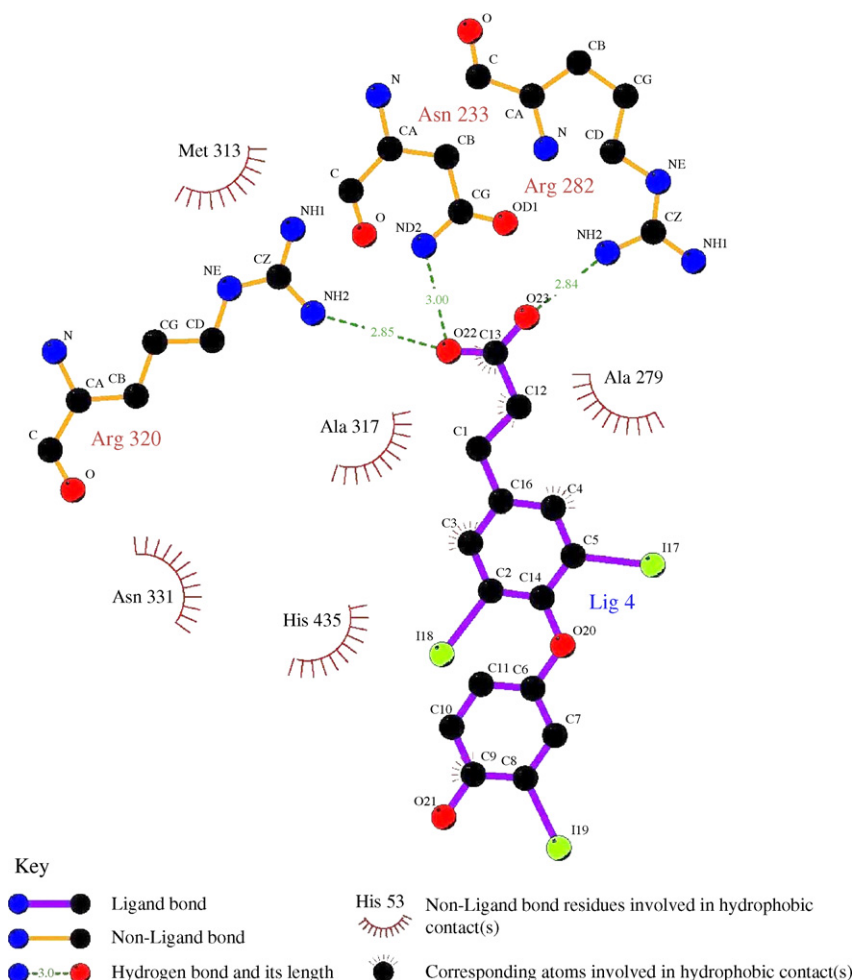


Fig. 4. Schematic representation of interaction between ligand 4 and the TRβ produced using the Ligplot program developed by Wallace et al. [40].

QSAR models using the standard implementation in the SYBYL package. Cross-validation in PLS was carried out using the leave-one-out option to obtain the optimal number of components to be used subsequently in the final analysis [32,38]. The cross-validated coefficient q^2 was calculated using Eq. (2):

$$q^2 = 1 - \frac{\sum (Y_{\text{predicted}} - Y_{\text{observed}})^2}{\sum (Y_{\text{observed}} - Y_{\text{mean}})^2} \quad (2)$$

where $Y_{\text{predicted}}$, Y_{observed} , and Y_{mean} were predicted, observed, and mean values of the target property, respectively. $(Y_{\text{predicted}} - Y_{\text{observed}})^2$ was the predictive sum of squares known as PRESS. In addition, the statistical significance of the models was described by the SEE and F and probability value computed according to the definitions in SYBYL. The final model was constructed with the optimum number of components equal to that yielding the highest q^2 .

3. Results and discussion

3.1. Docking analysis

Flexible docking of ligand 4, the most active compound among the whole data set, was carried out in the active site of the thyroid hormone receptor β . The best possible binding mode of ligand 4 in the TR β 1 active site was displayed in Fig. 3 and corresponding 2D interaction models were presented in Fig. 4. The predicted binding free energy of ligand 4 was -11.78 kcal/mol.

It can be seen clearly from Figs. 3 and 4 that the benzene ring A and B of ligand 4 are surrounded by hydrophobic residues Ala 279, Met 313, Ala 317, Asn 331 and His 435 mainly through the hydrophobic interaction. In addition, the two oxygen atoms of the terminal of B ring form three hydrogen bonds to Asn 233, Arg 282 and Arg 320 as hydrogen-bond acceptors. The results are in good agreement with the experimental conclusion of Malm's work [17].

3.2. 3D-QSAR models

3.2.1. CoMFA analysis

The 3D-QSAR, CoMFA and CoMSIA studies, were carried out based on the alignment of bioactive conformation obtained from docking. The whole data set was divided into a training set of 49 and a test set of 12 molecules at random so as to form the standard 4:1 training set to test set ratio for a QSAR study.

The CoMFA PLS analysis results were listed in Table 2 and Table 3. The model gives a cross-validated q^2 of 0.600 for six components and non-cross-validated r^2 of 0.974, F of 257.898, with a SEE of 0.195 and shows good predictive ability. The corresponding field contributions of steric and electrostatic are 35.9%, and 64.1%. These values suggest a good conventional statistical correlation as shown in Fig. 5(a), and a satisfactory predictive ability of the CoMFA model.

3.2.2. CoMSIA analysis

CoMSIA analysis results were also summarized in Table 2 and Table 3. A CoMSIA model with a cross-validated q^2 of 0.616 for six components and non-cross-validated r^2 of 0.974, F of 261.713 and SEE of 0.194 were obtained. Fig. 5(b) shows the relationship between the predicted and the experimental pIC_{50} values for the non-cross-validated analyses of CoMSIA model. The corresponding field contributions of variables are 7.8%, 29.7%, 17.7%, 25.5%, and 19.3%, respectively. The result indicate that electrostatic field is very important for CoMSIA model, which is in good agreement with the result in CoMFA analysis. In addition, CoMSIA analysis also reveals that the contribution of hydrogen-bond donor field is significant. The decrease of contribution of steric field in the CoMSIA model can be explained by the introducing of hydrophobic

Table 2

Predicted activities (PA) from CoMFA and CoMSIA models compared with the experimental activities (EA) and the errors

No.	pIC_{50}	CoMFA		CoMSIA	
		PA	Error	PA	Error
1	9.59	9.63	-0.04	9.33	0.26
2	10.32	10.31	0.01	10.46	-0.14
3	9.96	9.86	0.10	10.00	-0.04
4	10.72	10.62	0.10	10.70	0.02
5	10.60	10.34	0.26	10.45	0.15
6	8.68	8.90	-0.22	8.68	0.00
7*	10.02	9.21	0.81	9.51	0.51
8*	7.68	8.41	-0.73	7.82	-0.14
9	8.96	9.21	-0.25	8.94	0.03
10	9.82	9.98	-0.16	9.99	-0.17
11*	8.54	8.61	-0.07	8.65	-0.11
12	8.47	8.56	-0.09	8.65	-0.18
13	9.03	9.25	-0.21	9.17	-0.14
14	7.17	7.01	0.16	7.04	0.13
15	9.70	9.53	0.17	9.31	0.39
16	8.40	8.33	0.07	8.19	0.21
17	7.68	7.87	-0.19	8.02	-0.34
18	7.96	7.95	0.01	8.10	-0.14
19	9.11	9.04	0.07	9.31	-0.20
20*	8.47	8.34	0.13	8.50	-0.03
21	7.30	7.33	-0.03	7.36	-0.06
22	7.12	7.07	0.05	6.92	0.20
23	7.06	7.10	-0.04	7.02	0.04
24	6.86	6.96	-0.10	7.08	-0.22
25	7.39	7.41	-0.02	7.28	0.11
26*	6.91	7.17	-0.26	7.30	-0.39
27	7.17	7.07	0.10	7.09	0.09
28*	7.55	7.56	-0.01	7.85	-0.3
29*	8.11	7.97	0.14	8.30	-0.19
30	8.22	7.86	0.36	8.12	0.10
31	8.12	8.21	-0.09	8.14	-0.02
32	8.96	8.84	0.12	9.12	-0.16
33	8.02	8.03	-0.01	7.93	0.09
34*	7.22	8.22	-0.99	8.20	-0.98
35	7.08	6.94	0.14	7.09	-0.01
36	7.33	7.60	-0.27	7.55	-0.22
37	8.22	8.16	0.06	8.22	0.00
38	7.46	7.45	0.02	7.42	0.04
39	8.38	8.31	0.07	8.13	0.25
40	9.21	9.04	0.17	9.36	-0.15
41*	8.17	7.97	0.20	8.09	0.08
42*	7.74	7.79	-0.05	7.66	0.08
43	7.43	7.51	-0.08	7.45	-0.02
44	8.32	8.07	0.25	8.13	0.19
45	8.07	8.15	-0.08	8.08	-0.01
46*	9.33	8.52	0.81	8.23	1.10
47	7.17	7.44	-0.27	7.30	-0.13
48	8.46	8.27	0.19	8.33	0.13
49	6.85	6.89	-0.04	6.84	0.01
50	7.74	7.74	0.00	7.97	-0.23
51	8.37	8.44	-0.07	8.31	0.06
52	7.33	7.48	-0.15	7.43	-0.10
53	7.80	7.69	0.11	7.69	0.11
54	7.35	7.48	-0.13	7.44	-0.09
55	9.55	10.19	-0.64	9.79	-0.24
56	10.22	9.83	0.39	9.90	0.32
57	8.07	8.02	0.05	7.98	0.09
58	7.29	7.08	0.21	6.99	0.30
59	6.06	6.26	-0.20	6.56	-0.50
60	6.62	6.49	0.13	6.42	0.21
61*	7.82	8.07	-0.25	8.40	-0.58

* Test set.

field in the CoMSIA model and also by the fact that in some cases, the steric field is correlated to some extent with hydrophobic field.

3.2.3. Validation of the 3D-QSAR models

To validate the stability and predictive ability of the obtained models, 12 compounds not included in the construction of CoMFA and CoMSIA models were selected as the test set. The predicted

Table 3
The statistical parameters for the final CoMFA and CoMSIA model

Statistical parameters	CoMFA model	CoMSIA model
q^2_a	0.600	0.616
Number of molecules in training set	49	49
Number of molecules in test set	12	12
ONC ^b	6	6
r^2_c	0.974	0.974
SEE ^d	0.195	0.194
F_{ratio}^e	257.898	261.713
$r^2_{pred}^f$	0.688	0.674
Fraction of field contributions ^g		
Steric	0.359	0.078
Electrostatic	0.641	0.297
Hydrophobic		0.177
Donor		0.255
Acceptor		0.193

^a Cross-validated correlation coefficient.

^b Optimum number of components.

^c Non-cross-validated correlation coefficient.

^d Standard error of estimate.

^e F -test value.

^f Predictive r^2 .

^g Field contributions: steric; electrostatic; hydrophobic; hydrogen-bond donor; hydrogen-bond acceptor.

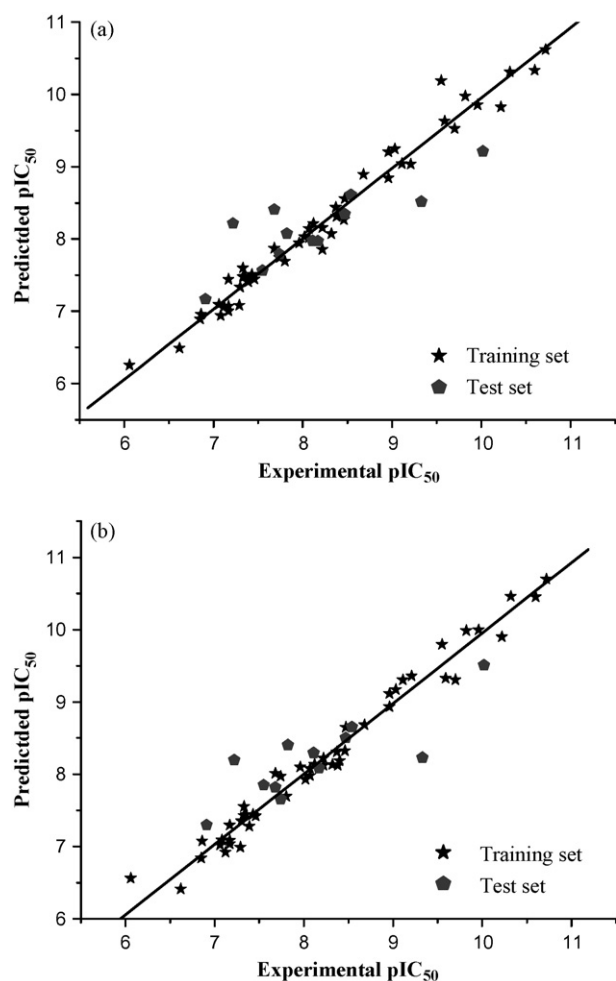


Fig. 5. Plot of the predicted pIC_{50} versus the experimental pIC_{50} values for the CoMFA model (a) and CoMSIA model (b).

results of the test set were also listed in Table 2 (asterisk labeled) and shown in Fig. 5. It can be seen clearly from Fig. 5 that the predicted pIC_{50} values of the test set compounds are in good agreement with the experimental data in a tolerable error range, with r^2 of 0.688 and 0.674 for CoMFA and CoMSIA models, respectively. Testing results also indicate that the CoMFA and CoMSIA models could be reliably used to design novel agonist with desired activity for the TR β . Compared with the former quantitative structure-activity relationship models [20–23], the 3D-QSAR models give more information about the structure-activity relationship and can be conveniently visualized.

3.2.4. CoMFA and CoMSIA contour maps

To visualize the information content of the derived 3D-QSAR models, CoMFA and CoMSIA contour maps were generated. The field energies at each lattice point were calculated as the scalar results of the coefficient and the standard deviation associated with a particular column of the data table ("stdev*coeff"), which was always plotted as the percentage of the contribution to the CoMFA or CoMSIA equation.

The CoMFA contour maps of steric and electrostatic field are shown in Fig. 6. In the CoMFA steric field, the green contours (contribution level of 80%) represent a steric group that confers an increased activity while yellow contours (contribution level of 20%) represent a bulky group that results in a decreased activity. Similarly, the blue contours indicate regions where the addition of electropositive substituents increases activity (contribution level of 80%); red indicates regions where the addition of electronegative substituents increases activity (contribution level of 20%). Compound 4 is displayed in the map in aid of visualization.

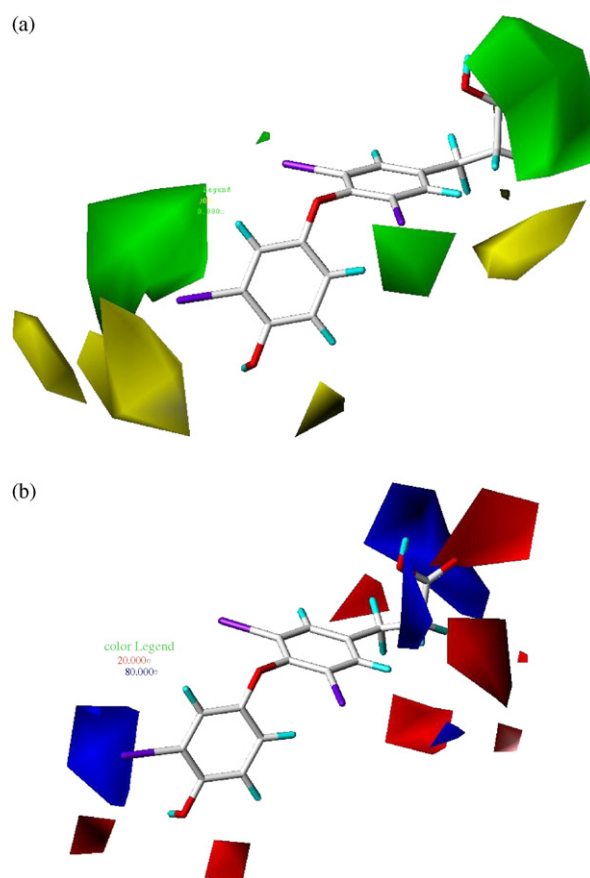


Fig. 6. CoMFA StDev * Coeff contour plots. (a) Contour maps for steric field and (b) contour maps for electrostatic field.

In Fig. 6(a), the contour map of the steric field of CoMFA model, a large region of green contour near the *meta* position of the A ring indicates that steric bulk is favored there. A large region of yellow contour near the *para* position of A ring suggest that bulky group would decrease the activity. The activity of compounds 49–54 all decreased after the –OH groups on that position were replaced with bulky groups. A small region of green contour around the *ortho* position of the B ring suggests that steric bulk is favored there. For example, the activity of compound 6 (–Br) was shown to be higher than that of compound 8 (–Cl). This can also be shown by

the order for the activity of other compounds, such as activity of compounds 7(–Br) > 9(–Cl); 40(–Br) > 48(–Cl); 77(–Br) > 78(–Cl). A large region of green contour around the carboxyl of benzene ring B represent that bulky group would enhance the activity. This can be explained by the fact that replacement of this position with $-(CH_2)_2CO_2H$ group enhances the binding affinity ($4 > 2$; $5 > 6$).

In the contour map of the electrostatic field of CoMFA model, shown in Fig. 6(b), a large area of blue contour around the *meta* position of the A ring indicate that electropositive substituents are favored there. It can explain the fact that the activity of compounds

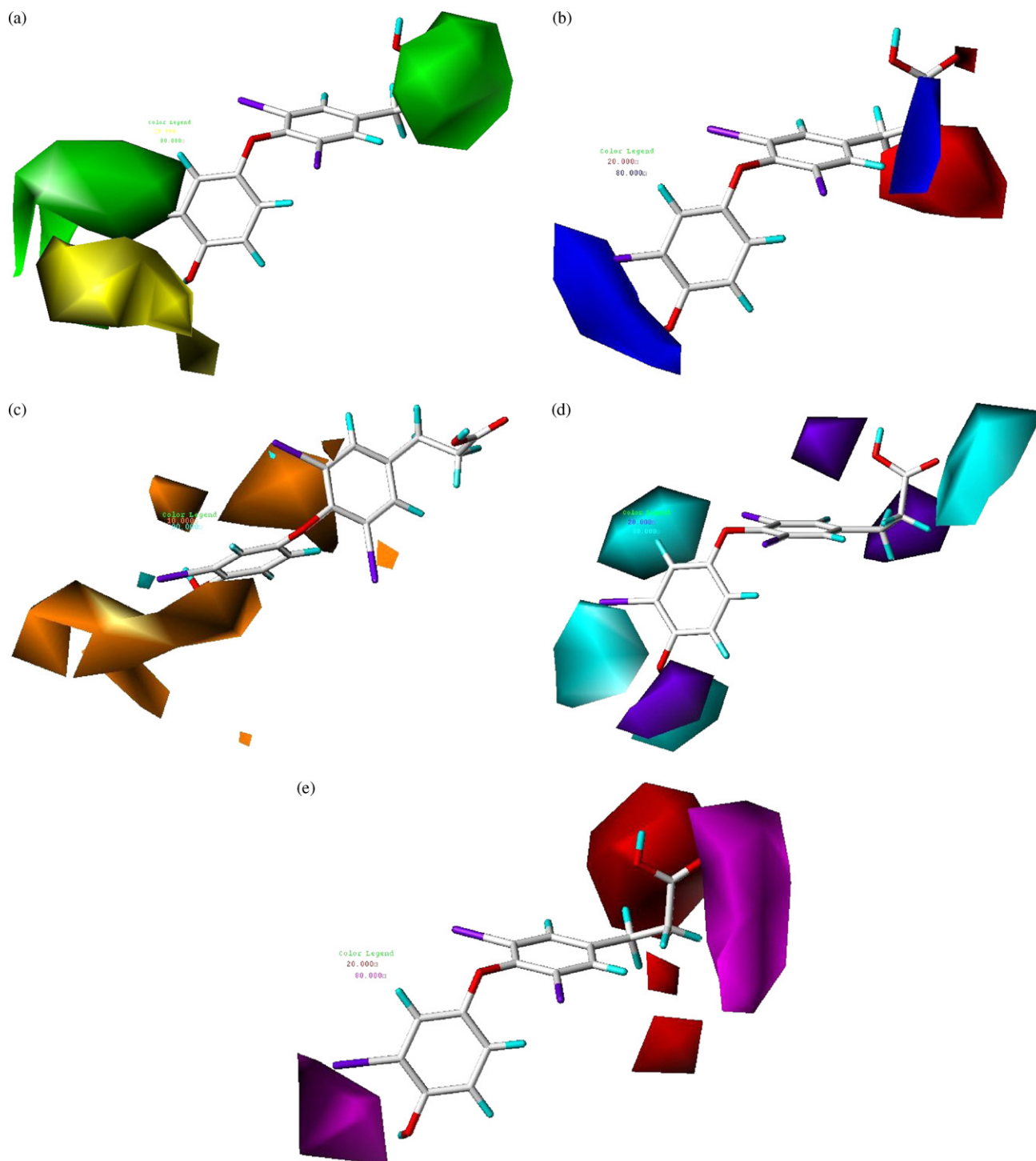


Fig. 7. CoMSIA StDev * Coeff contour plots. (a) Contour maps for steric field; (b) contour maps for electrostatic field; (c) contour maps for hydrophobic field; (d) contour maps for H-bond donor field and (e) contour maps for H-bond acceptor field.

3 (-Isopropyl) and 15 (3-Et) are higher than that of the corresponding compounds 1 (-I) and 13 (3-CF₃). A large region of blue contour near the carboxyl of benzene ring B suggests that electropositive substituents would increase the activity. This is in agreement with the fact that the binding affinity of compounds 4 and 5 with -NH₂ group substituted by hydrogen atom is higher than that of the compounds 1 and 3. A red area near the terminal of the carboxyl of benzene ring B indicates that electronegative substituents are favored there. Therefore, the carboxyl of benzene ring B is an important group to maintain their binding affinity.

The steric and electrostatic field distributions of CoMSIA, depicted in Fig. 7(a) and (b), are generally in accordance with the field distributions of CoMFA map (Fig. 6(a) and (b)). The hydrophobic contour map of CoMSIA model is displayed in Fig. 7(c). Cyan (contribution level of 90%) and orange (contribution level of 10%) contours indicate the regions where hydrophobic and hydrophilic groups were preferred, respectively. A small cyan contour map around the *meta* position of the A ring indicate that hydrophobic groups would be favorable for binding activity. The large orange contour map located around the *para* position of A ring suggest that hydrophobic groups at these position would decrease the binding affinity. As a consequence when the -OH group on the *para* position A ring were replaced with hydrophobic groups, it shows reduction in activity. This can be seen from compounds 49–54 in which the -OH on that position replaced with hydrophobic groups result in a decrease of activity as compared to compound 9.

The CoMSIA contour map of the hydrogen-bond donor and hydrogen-bond acceptor field are shown in Fig. 7(d) and (e), respectively. Cyan contours (contribution level of 80%) indicate regions where H-bond donor group increases activity, purple contours (contribution level of 20%) suggest regions where H-bond donor group decreases activity. A purple contour near the *para* position of A ring suggest that H-bond donor groups are disfavored there, which is consistent well with the results of the docking study that the oxygen atom at this position forms a hydrogen bond with His 435 as hydrogen acceptor. Magenta contours (contribution level of 80%) indicate regions where H-bond acceptor group increases activity; red contours (contribution level of 20%) represent region where H-bond acceptor group decreases activity. The results obtained from Fig. 7(d) and (e) are in accordance with the results of docking study.

4. Conclusions

In this study, we have established predictive CoMFA and CoMSIA 3D-QSAR models for the TR β agonists. The 3D-QSAR approach has revealed the importance of the shapes of different groups in influencing binding affinities to be determined. The results of CoMSIA 3D-QSAR model perform better than that of CoMFA. Molecular docking has been employed to identify a potential binding mode for these agonist ligands at TR β active site. The results of this study can provide further support to the structure-based design of agonist compounds acting as potential drugs for non-thyroid disorders.

Acknowledgement

This work was supported by the Program for New Century Excellent Talents in University (No. NCET-07-0399).

Appendix A. Supplementary data

Supplementary data associated with this article can be found, in the online version, at doi:10.1016/j.jmgm.2008.03.003.

References

- [1] M.A. Lazar, Thyroid hormone receptors: multiple forms, multiple possibilities, *Endocr. Rev.* 14 (1993) 184–193.
- [2] R.H. Zetterström, L. Solomin, L. Jansson, B.J. Hoffer, L. Olson, T. Perlmann, Dopamine neuron agenesis in Nurr1-deficient mice, *Science* 276 (1997) 248–250.
- [3] E.D. Bischoff, M.M. Gottardis, T.E. Moon, R.A. Heyman, W.W. Lamph, Beyond tamoxifen: the retinoid X receptor-selective ligand Igd1069 (targretin) causes complete regression of mammary carcinoma, *Cancer Res.* 58 (1998) 479–484.
- [4] E. Elstner, C. Muller, K. Koshizuka, E.A. Williamson, D. Park, H. Asou, P. Shintaku, J.W. Said, D. Heber, H.P. Koeffler, Ligands for peroxisome proliferator-activated receptor gamma and retinoic acid receptor inhibit growth and induce apoptosis of human breast cancer cells in vitro and in BNX mice, *Proc. Natl. Acad. Sci.* 95 (1998) 8806–8811.
- [5] M. Shiohara, M.I. Dawson, P.D. Hobbs, N. Sawai, T. Higuchi, K. Koike, A. Komiyama, H.P. Koeffler, Effects of novel RAR- and RXR-selective retinoids on myeloid leukemic proliferation and differentiation in vitro, *Blood* 93 (1999) 2057–2066.
- [6] A.N. Fanjul, F.J. Piedrafita, H. Al-Shamma, M. Pfahl, Apoptosis Induction, Potent antiestrogen receptor-negative breast cancer activity in vivo by a retinoid antagonist, *Cancer Res.* 58 (1998) 4607–4610.
- [7] A. Loireau, N. Autissier, P. Dumas, O. Michael, E.C. Jorgensen, R. Michael, Comparative effects of 3,5-dimethyl-3'-isopropyl-L-thyronine (DIMIT) and 3,5-diiodo-3'-isopropylthiyoacetic acid (IpTA2) on body weight gain and lipid metabolism in genetically obese Zucker rats, *Biochem. Pharmacol.* 35 (1986) 1691–1696.
- [8] S.F. Engelken, R.P. Eaton, The effects of altered thyroid status on lipid metabolism in the genetic hyperlipemic Zucker rat, *Atherosclerosis* 38 (1981) 177–188.
- [9] P. Hansson, S. Valdemarsson, P. Nilsson-Ehle, Experimental hyperthyroidism in man: effects on plasma lipoproteins, lipoprotein lipase and hepatic lipase, *Horm. Metab. Res.* 15 (1983) 449–452.
- [10] L. Scarabottolo, E. Trezzi, P. Roma, A.L. Catapano, Experimental hypothyroidism modulates the expression of low-density lipoprotein receptor by the liver, *Atherosclerosis* 59 (1986) 329–333.
- [11] D. Forrest, B. Vennström, Functions of thyroid hormone receptors in mice, *Thyroid* 10 (2000) 41–52.
- [12] K. Takeda, A. Sakurai, L.J. DeGroot, S. Refetoff, Recessive inheritance of thyroid hormone resistance caused by complete deletion of the protein-coding region of the thyroid hormone receptor- α gene, *J. Clin. Endocrin. Metab.* 74 (1992) 49–55.
- [13] A.H. Underwood, J.C. Emmett, D. Ellis, S.B. Flynn, P.D. Leeson, G.M. Benson, R. Novelli, N.J. Pearce, V.P. Shah, A thyromimetic that decreases plasma cholesterol levels without increasing cardiac activity, *Nature* 324 (1986) 425–429.
- [14] N.H. Nguyen, J.W. Apriletti, S.T. Cunha Lima, P. Webb, J.D. Baxter, T.S. Scanlan, Rational design and synthesis of a novel thyroid hormone antagonist that blocks coactivator recruitment, *J. Med. Chem.* 45 (2002) 3310–3320.
- [15] R.L. Dow, S.R. Schneider, E.S. Paight, R.F. Hank, P. Chiang, P. Cornelius, E. Lee, W.P. Newsome, A.G. Swick, J. Spitzer, D.M. Hargrove, T.A. Patterson, J. Pandit, B.A. Chrunk, P.K. LeMotte, D.E. Danley, M.H. Rosner, M.J. Ammirati, S.P. Simons, G.K. Schulte, B.F. Tate, P. DaSilva-Jardine, Discovery of a novel series of 6-azauracil-based thyroid hormone receptor ligands: potent, TR[β] subtype-selective thyromimetics, *Bioorg. Med. Chem. Lett.* 13 (2003) 379–382.
- [16] S. Borngräber, M.-J. Budny, G. Chiellini, S.T. Cunha-Lima, M. Togashi, P. Webb, J.D. Baxter, T.S. Scanlan, R.J. Fletterick, Ligand selectivity by seeking hydrophobicity in thyroid hormone receptor, *Proc. Natl. Acad. Sci.* 100 (2003) 15358–15363.
- [17] J. Malm, G.J. Grover, M. Farnegårdh, Recent advances in the development of agonists selective for β 1-type thyroid hormone receptor, *Mini-Rev. Med. Chem.* 7 (2007) 79–86.
- [18] Y. Liu, Y.L. Li, K. Mellström, C. Mellin, L.G. Bladh, K. Koehler, N. Garg, A.M. Garcia Collazo, C. Litten, B. Husman, K. Persson, J. Ljunggren, G. Grover, P.G. Sleph, R. George, J. Malm, Thyroid receptor ligands. 1. Agonist ligands selective for the thyroid receptor beta 1, *J. Med. Chem.* 46 (2003) 1580–1588.
- [19] J.J. Hangeland, A.M. Dowsky, T. Dejneka, T.J. Friends, P. Devasthale, K. Mellström, J. Sandberg, M. Grynfarb, J.S. Sack, H. Einspahr, M. Farnegårdh, B. Husman, J. Ljunggren, K. Koehler, C. Sheppard, J. Malm, D.E. Ryono, Thyroid receptor ligands. Part 2: Thyromimetics with improved selectivity for the thyroid hormone receptor beta, *Bioorg. Med. Chem. Lett.* 14 (2004) 3549–3553.
- [20] A. Hedfors, T. Appelqvist, B. Carlsson, L.G. Bladh, C. Litten, P. Agback, M. Grynfarb, K.F. Koehler, J. Malm, Thyroid receptor ligands. 3. Design and synthesis of 3,5-Dihalo-4-alkoxyphenylalkanoic acids as indirect antagonists of the thyroid hormone receptor, *J. Med. Chem.* 48 (2005) 3114–3117.
- [21] A.M. Garcia Collazo, K.F. Koehler, N. Garg, M. Farnegårdh, B. Husman, Y. Liu, J. Ljunggren, K. Mellström, J. Sandberg, M. Grynfarb, H. Ahola, J. Malm, Thyroid receptor ligands. Part 5: Novel bicyclic agonist ligands selective for the thyroid hormone receptor [beta], *Bioorg. Med. Chem. Lett.* 16 (2006) 1240–1244.
- [22] Y.L. Li, C. Litten, K.F. Koehler, K. Mellström, N. Garg, A.M. Garcia Collazo, M. Farnegårdh, M. Grynfarb, B. Husman, J. Sandberg, J. Malm, Thyroid receptor ligands. Part 4: 4'-amido bioisosteric ligands selective for the thyroid hormone receptor beta, *Bioorg. Med. Chem. Lett.* 16 (2006) 884–886.
- [23] K. Koehler, S. Gordon, P. Brandt, B. Carlsson, A. Backsbro-Saeidi, T. Appelqvist, P. Agback, G.J. Grover, W. Nelson, M. Grynfarb, M. Farnegårdh, S. Rehnmark, J. Malm, Thyroid Receptor Ligands. 6. A high affinity "Direct Antagonist" selective for the thyroid hormone receptor beta, *Bioorg. Med. Chem. Lett.* 49 (2006) 6635–6637.
- [24] J. Malm, S. Gordon, P. Brandt, B. Carlsson, P. Agback, A. Backsbro Saeidi, J. Sandberg, Thyroid receptor ligands. Part 7: Indirect antagonists of the thyroid hormone receptor with improved affinity, *Bioorg. Med. Chem. Lett.* 17 (2007) 2018–2021.

- [25] G.J. Grover, J. Malm, Selective thyroid hormone agonists: a strategy for treating metabolic syndrome, *Drug Discov. Today: Ther. Strategies* 2 (2005) 137–142.
- [26] J. Malm, Thyroid hormone ligands and metabolic diseases, *Curr. Pharm. Des.* 10 (2004) 3525–3532.
- [27] Y. Ren, H. Liu, S. Li, X. Yao, M. Liu, Prediction of binding affinities to b1 isoform of human thyroid hormone receptor by genetic algorithm and projection pursuit regression, *Bioorg. Med. Chem. Lett.* 17 (2007) 2474–2482.
- [28] H. Liu, P. Gramatica, QSAR study of selective ligands for the thyroid hormone receptor b, *Bioorg. Med. Chem.* 15 (2007) 5251–5261.
- [29] A. Vedani, M. Dobler, M.A. Lill, The challenge of predicting drug toxicity in silico, *Basic Clin. Pharmacol. Toxicol.* 99 (2006) 187–194.
- [30] A. Vedani, M. Zumstein, M.A. Lill, B. Ernst, Simulating/selectivity at the human thyroid hormone receptor: consensus scoring using multidimensional QSAR, *Chem. Med. Chem.* 2 (2007) 78–87.
- [31] R.D. Cramer 3rd, D.E. Patterson, J.D. Bunce, Comparative molecular field analysis (CoMFA). 1. Effect of shape on binding of steroids to carrier proteins, *J. Am. Chem. Soc.* 110 (1988) 5959–5967.
- [32] R.D. Cramer 3rd, J.D. Bunce, D.E. Patterson, Crossvalidation, bootstrapping, and partial least squares compared with multiple regression in conventional QSAR studies, *Quant. Struct. Act. Relat.* 7 (1988) 18–25.
- [33] G. Klebe, U. Abraham, T. Mietzner, Molecular similarity indices in a Comparative Analysis (CoMSIA) of drug molecules to correlate and predict their biological activity, *J. Med. Chem.* 37 (1994) 4130–4146.
- [34] Sybyl version 6.9, Tripos Associates, St. Louis (MO) (1999).
- [35] G.M. Morris, D.S. Goodsell, R.S. Halliday, R. Huey, W.E. Hart, R.K. Belew, A.J. Olson, Automated docking using a Lamarckian genetic algorithm and an empirical binding free energy function, *J. Comput. Chem.* 19 (1998) 1639–1662.
- [36] S. Wold, A. Ruhe, H. Wold, W.J.I. Dunn, The covariance problem in linear regression. The partial least squares (PLS) approach to generalized inverses, *SIAM J. Sci. Stat. Comput.* 5 (1984) 735–743.
- [37] S. Wold, C. Albano, W.J. Dunn, U. Edlund, K. Esbenson, P. Geladi, S. Hellberg, W. Lindberg, M. Sjostrom, in: B. Kowalski (Ed.), *Chemometrics: Mathematics and Statistics in Chemistry*, Reidel, Dordrecht, The Netherlands, 1984, pp. 17–95.
- [38] S. Wold, Cross validation estimation of the number of components in factor and principal components models, *Technometrics* 4 (1978) 397–405.
- [39] W.L. DeLano, The PyMOL Molecular Graphics System, DeLano Scientific, Palo Alto, CA, USA, 2002.
- [40] A.C. Wallace, R.A. Laskowski, J.M. Thornton, LIGPLOT: a program to generate schematic diagrams of protein-ligand interactions, *Prot. Eng.* 8 (1995) 127–134.